

Provided for non-commercial research and education use.  
Not for reproduction, distribution or commercial use.

Volume 405, Issue 14, 15 July 2010 ISSN 0921-4526



**PHYSICA** **B**  
CONDENSED MATTER



Recognized by the European Physical Society



ETOPIM 8  
JUNE 7-12, 2009  
RETHYMNON, CRETE

Proceedings of the Eighth International  
Conference on Electrical Transport and  
Optical Properties of Inhomogeneous  
Media

**ETOPIM-8**

held in Rethymnon, Crete, Greece  
7-12 June 2009

Guest Editors:  
Costas Soukoulis  
Maria Kafesaki

Available online at [www.sciencedirect.com](http://www.sciencedirect.com)  
 ScienceDirect

<http://www.elsevier.com/locate/physb>

This article appeared in a journal published by Elsevier. The attached copy is furnished to the author for internal non-commercial research and education use, including for instruction at the authors institution and sharing with colleagues.

Other uses, including reproduction and distribution, or selling or licensing copies, or posting to personal, institutional or third party websites are prohibited.

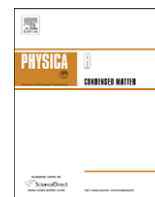
In most cases authors are permitted to post their version of the article (e.g. in Word or Tex form) to their personal website or institutional repository. Authors requiring further information regarding Elsevier's archiving and manuscript policies are encouraged to visit:

<http://www.elsevier.com/copyright>



Contents lists available at ScienceDirect

Physica B

journal homepage: [www.elsevier.com/locate/physb](http://www.elsevier.com/locate/physb)

## A network model for electrical transport in sea ice

J. Zhu, K.M. Golden\*, A. Gully, C. Sampson

University of Utah, Department of Mathematics, 155 S 1400 E RM 233, Salt Lake City, UT 84112-0090, USA

### ARTICLE INFO

#### Keywords:

Sea ice  
Electrical conductivity  
Network model  
Sea ice thickness

### ABSTRACT

Monitoring the thickness of sea ice is an important tool in assessing the impact of global warming on Earth's polar regions, and most methods of measuring ice thickness depend on detailed knowledge of its electrical properties. We develop a network model for the electrical conductivity of sea ice, which incorporates statistical measurements of the brine microstructure. The numerical simulations are in close agreement with direct measurements we made in Antarctica on the vertical conductivity of first year sea ice.

© 2010 Elsevier B.V. All rights reserved.

### 1. Introduction

Sea ice is a critical component of Earth's climate system as well as a sensitive indicator of climate change. Determining the thickness distribution of the polar sea ice packs is a central problem in monitoring the impact of global warming. However, there is significant uncertainty in our knowledge of the ice thickness distribution and how it is changing. Not only does this uncertainty affect assessments of how the changing climate is impacting the polar regions, but it also affects predictions of global climate models, where accurate knowledge of sea ice initial conditions is essential for long term simulations.

Most methods of measuring sea ice thickness, and interpretation of the data obtained, depend on detailed knowledge of the electrical properties of the ice. Since sea ice is a composite of pure ice with brine inclusions [21,3], whose volume fraction and geometry depend strongly on temperature, understanding its electrical properties is a challenging problem in the theory of inhomogeneous materials. While the electrical conductivity of pure ice is negligible for most purposes, the electrical conductivity of brine can be substantial. Here we develop a network model for the electrical conductivity of sea ice, and compare the results with direct measurements of the vertical conductivity of first year sea ice we made during the 2007 Sea Ice Physics and Ecosystem eXperiment (SIPEX) expedition off the coast of East Antarctica, from the Australian icebreaker *Aurora Australis* [9].

Early DC resistivity measurements on sea ice were aimed at determining ice thickness [5,19,20]. Initially all these studies employed surface soundings using 4 electrodes in either the Wenner or Schlumberger configurations, although Thyssen et al.

[19] later used vertically arranged electrodes in the side of an ice pit. Later measurements in the Antarctic were also reported [2]. The anisotropic nature of the resistivity of sea ice, due to the preferential vertical alignment and connectivity of brine pores, leads to such measurements significantly underestimating the ice thickness.

More promising determinations of sea ice thickness have been achieved using low frequency electromagnetic (EM) techniques [14,11,13,22,17]. The technique relies on a time varying primary magnetic field (generated by a transmitter coil) inducing eddy currents in the seawater beneath the comparatively resistive ice. The secondary magnetic field produced is sensed by a receiver coil, determining an apparent conductivity which results essentially from an integration over the vertical distance between the instrument and induced currents. The thickness is found using empirical relationships [12], with good results for smooth ice and underestimates near ridges [12]. The technique is adaptable to continuous measurements being made either from a helicopter or ship [11].

Previous measurements of the conductivity of sea ice relied almost exclusively on indirect methods which mix the horizontal and vertical components. Moreover, these indirect means make it difficult to accurately recover the dependence of the conductivity on the properties of the brine microstructure, namely, its brine volume fraction  $\phi$ , which depends on the temperature  $T$  and salinity  $S$  of the ice [4,21,3]. During the 2007 Australian SIPEX expedition, Golden and Gully extracted cylindrical cores of sea ice and made vertical conductivity measurements along these cores using metal probes attached to a Yew Earth Resistance Tester, as described in Ref. [9]. We also measured salinity and temperature along each core in order to relate the electrical measurements to microstructural data [15,7,8,16], such as the brine volume fraction.

Part of our motivation for focusing on the vertical component of the electrical conductivity is that it is closely related to the vertical component of the fluid permeability of sea ice. Fluid

\* Corresponding author.

E-mail addresses: [zhu@math.utah.edu](mailto:zhu@math.utah.edu) (J. Zhu), [golden@math.utah.edu](mailto:golden@math.utah.edu) (K.M. Golden), [gully@math.utah.edu](mailto:gully@math.utah.edu) (A. Gully), [christian.sampson@gmail.com](mailto:christian.sampson@gmail.com) (C. Sampson).

transport in sea ice mediates a broad range of processes such as the growth and decay of seasonal ice, the evolution of melt ponds which determine ice pack albedo, and biomass build-up [8,6]. Our work here will help lay the foundation for electrically monitoring fluid transport in sea ice. In fact, the random resistor network model we develop here is based on the random pipe network we used previously to model the fluid permeability of sea ice [23]. Statistical information about the brine microstructure [15,7,8,16] is used to determine the statistical distributions of the resistors in the electrical network.

## 2. The network model for the effective conductivity of sea ice

In this model, we consider a piece of sea ice with brine inclusions specified by a brine volume fraction  $\phi$  and other statistical assumptions, and focus on the effect of the brine structure on electrical conduction in the material. More specifically, we study the behavior of the effective vertical conductivity and its dependence on the brine inclusions. Let  $\Phi$  be the electric potential, and  $\sigma$  the local conductivity tensor, which depends on the brine volume fraction. Since the current density  $J$  is related to the electric potential through  $J = -\sigma \nabla \Phi$ , and assuming the material is free of electric charge, the equation for electrical conduction is

$$\nabla \cdot \sigma \nabla \Phi = 0. \quad (1)$$

This is similar to the incompressible fluid permeability equation for the pressure from Darcy's law,

$$\nabla \cdot \mathbf{k} \nabla p = 0, \quad (2)$$

where  $p$  is the incompressible fluid pressure and  $\mathbf{k}$  is the permeability tensor.

Here we define the effective conductivity  $\sigma_v^*$  of the sea ice structure in the vertical direction through

$$J_z = -\sigma_v^* \frac{\Delta \Phi}{\Delta z} \quad (3)$$

for the current density  $J_z$  in  $z$  direction, and the potential difference  $\Delta \Phi$  over a thickness  $\Delta z$ .

To simulate the electric field through the conducting microstructure of sea ice, consider an ice sheet of depth  $D$ , similar to the structure used in Ref. [23]. Take a thin vertical slice of horizontal thickness  $h$  and length span  $L$ . We model this ice sheet by a two dimensional lattice of nodes connected by conducting tubes, as shown in Fig. 1. The slice has a rectangular  $L \times D$  vertical cross section, which is divided into a grid with  $m$  equally spaced sections in the horizontal direction and  $n$  equally spaced sections

in the vertical direction, so that  $L/m = D/n = h$ , for some large integers  $m$  and  $n$ . The model parameter  $h$  can be viewed as the dimension of a cell in which a typical brine inclusion is contained. In this network model,  $h$  will be chosen according to the sea ice we simulate, its brine volume fraction, and our computing capacities. The tubes are assumed to have circular shapes with different radii, and the current through the medium is induced by an electric potential drop  $\Delta \Phi = \Phi_t - \Phi_b$ , where  $\Phi_b$  and  $\Phi_t$  are the potentials at the bottom and the top of the sea ice sample, with the assumption that  $\Phi_b > \Phi_t$  so there is an upward current flow in the medium. The cross sectional areas of the tubes chosen below generate fluid pores comparable to the brine inclusions found in young sea ice. The lattice nodes are the vertices  $(i, j)$ ,  $0 \leq i \leq m, 0 \leq j \leq n$ , of a rectangular grid, as in Fig. 1(a). Nearest neighbors are connected by vertical and horizontal tubes, with a potential  $\Phi_{ij}$  defined at each node  $(i, j)$ . To each node  $(i, j)$  with  $0 \leq i \leq m-1, 0 \leq j \leq n-1$ , the horizontal tube to the right of  $(i, j)$  has radius  $R = R_{ij}^h$ , and the vertical tube on top of  $(i, j)$  has radius  $R = R_{ij}^v$ , as shown in Fig. 1(b).

Since the brine conductivity is substantially higher than the conductivity of the surrounding ice (on the order of  $10^8$ ), we can assume that electrical conduction takes place mostly through the brine tubes. The effect of negligible conduction through pure ice will be modeled by adding a simple conducting component to the system. Unlike the permeability model, where the fluid flux depends only on the brine geometry, electrical conduction in the microstructure includes a temperature dependent local conductivity. For each tube of radius  $R$  connecting two nodes with a uniform conductivity  $\sigma_{tube}$ , the electric current through the tube can be established based on the voltage drop and the cross sectional area  $A$  as follows:

$$I = \sigma_{tube} A E = -\sigma_{tube} \pi R^2 \nabla \Phi, \quad (4)$$

where  $\Phi$  is the electric potential,  $E$  is the electric field and  $R$  is the radius of the tube. For each tube connecting two neighboring nodes, the potential gradient can be well approximated by the potential drop divided by the spacing  $h$ . Given the potentials at neighboring nodes, different currents converging to the node  $(i, j)$  can be easily computed, and they must balance due to Kirckoff's law. Let  $\sigma_{ij}^h$  and  $\sigma_{ij}^v$  denote the brine conductivity for the tubes to the right and on the top of node  $(i, j)$ , respectively. This leads to the following equations,

$$\begin{aligned} \sigma_{ij}^v (R_{ij}^v)^2 (\Phi_{i,j+1} - \Phi_{ij}) + \sigma_{i,j-1}^v (R_{i,j-1}^v)^2 (\Phi_{i,j-1} - \Phi_{ij}) \\ + \sigma_{ij}^h (R_{ij}^h)^2 (\Phi_{i+1,j} - \Phi_{ij}) + \sigma_{i-1,j}^h (R_{i-1,j}^h)^2 (\Phi_{i-1,j} - \Phi_{ij}) = 0, \end{aligned} \quad (5)$$

for  $i = 1, \dots, m-1$ , and  $j = 1, \dots, n-1$ , with appropriate modifications on the edges of the lattice. Notice that this equation is similar to the equation derived for the fluid permeability model [23]:

$$\begin{aligned} (R_{ij}^v)^4 (p_{i,j+1} - p_{ij}) + (R_{i,j-1}^v)^4 (p_{i,j-1} - p_{ij}) \\ + (R_{ij}^h)^4 (p_{i+1,j} - p_{ij}) + (R_{i-1,j}^h)^4 (p_{i-1,j} - p_{ij}) = 0, \end{aligned} \quad (6)$$

where  $p_{ij}$  is the pressure at node  $(i, j)$ . We remark that in the conductivity model the coefficients depend on the radius ( $\sim R^2$ ) not as strongly as in the permeability case ( $\sim R^4$ ). On the other hand, here the local brine conductivity depends on temperature and salinity, and it could have spatial variations once we allow the temperature and salinity to be spatially non-uniform.

The boundary conditions for  $\Phi$  are prescribed so that  $\Phi$  is periodic in the horizontal direction with period  $L$ , and it satisfies Dirichlet conditions at the top and bottom of the region as

$$\Phi_{i,n} = \Phi_t, \quad \Phi_{i,0} = \Phi_b. \quad (7)$$

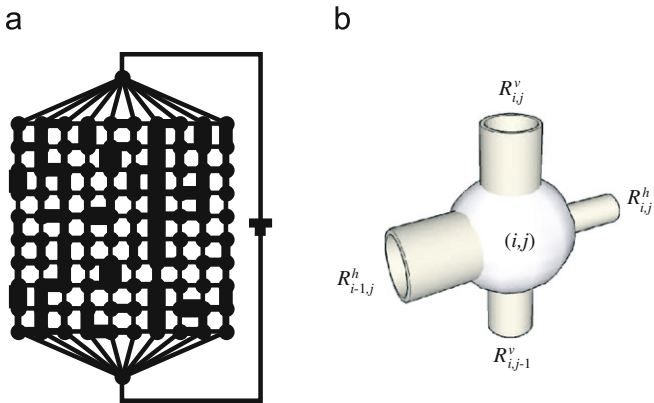


Fig. 1. (a) Random resistor network and (b) close-up of a node and adjoining conducting elements.

The total current through the brine network system can be obtained by adding currents through all the branches of the top layer,

$$I_{brine} = \pi \sum_{i=0}^m \sigma_{i,n-1}^v (R_{i,n-1}^v)^2 \frac{\Phi_{i,n-1} - \Phi_t}{h}. \quad (8)$$

The small effect of additional conduction through pure ice can be modeled as a current flow through another medium in parallel to the brine network,

$$I_{pure\ ice} = \sigma_{ice} L h (1 - \beta) \frac{\Phi_b - \Phi_t}{D}. \quad (9)$$

Here we introduce a coefficient  $\beta$  that models the loss of ice surface/volume for conduction due to the brine inclusions. It should be pointed out that due to the small ratio  $\sigma_{ice}/\sigma_b$  and the fact that  $\sigma_{ice}$  has a non-negligible temperature dependence, modifications due to  $\beta$  can be ignored in our study of the effective vertical conductivity.

With the introduction of the effective vertical conductivity for this composite in Eq. (3), and the relation between the current and current density,

$$J_z = \sigma_v^* \frac{\Phi_b - \Phi_t}{D} = \frac{I_{brine} + I_{pure\ ice}}{Lh}, \quad (10)$$

we have the effective conductivity

$$\sigma_v^* = \frac{\pi D}{Lh^2} \sum_{i=0}^m \sigma_{i,n-1}^v (R_{i,n-1}^v)^2 \frac{\Phi_{i,n-1} - \Phi_t}{\Phi_b - \Phi_t} + (1 - \beta) \sigma_{ice}. \quad (11)$$

The effect of  $\beta$  is ignored by setting it to zero in this study.

The multigrid algorithm to solve the system of equations (6) can be modified to solve the system of equations (5), and the numerical convergence is faster due to the coefficient dependence change from  $R^4$  to  $R^2$ .

### 3. Sea ice microstructure and numerical results

In this work, the microstructure of the sea ice slice is described as a collection of tubes with cross sectional areas sampled from a lognormal distribution that subsequently lead to a specified average brine volume fraction  $\phi$ , with parameters based on measurements of brine inclusions in first year sea ice [15,1]. Specifically, we sample the radius  $R$  so that  $\log A = \log(\pi R^2)$  is normally distributed with mean  $\mu$  and variance  $\alpha^2$ . We also assume that all the random radii are independent from each other. Given a particular sample of the tube radii, the brine volume fraction  $\phi$  of the slice can be readily computed by

$$\phi = \frac{\pi}{LD} \left( \sum_{i=0}^{m-1} \sum_{j=0}^n (R_{ij}^h)^2 + \sum_{i=0}^m \sum_{j=0}^n (R_{ij}^v)^2 \right). \quad (12)$$

The brine conductivity for each tube is determined by the temperature and the salinity of the sample under consideration, and it is assumed to remain the same value  $\sigma_b$  for all tubes in the sample for this model. The goal of this study is to investigate the dependence of the effective vertical conductivity  $\sigma_v^*$ , and the form factor  $\sigma_v^*/\sigma_b$ , on the porosity  $\phi$ , which is connected to the microstructure through Eq. (12). For consistency, it is necessary to choose the parameters  $\mu$  and  $\alpha$  such that the desired volume fraction is obtained, and that the statistical properties of the actual sea ice are reasonably matched. To this end, we first notice that given our assumption about the distribution of  $\log A$ , the expected value of the cross sectional area

$$E[A] = e^{\mu + 1/2\alpha^2}. \quad (13)$$

This should be matched to an interpolation of measured averages for the cross sectional area  $A$  as a function of brine volume

fraction  $\phi$  [10],

$$\langle A \rangle = \theta(\phi) = \pi(7 \times 10^{-5} + 1.6 \times 10^{-4} \phi)^2 \text{ m}^2. \quad (14)$$

This function approximates the dependence of the mean cross sectional area on the brine volume fraction  $\phi$  observed by Perovich and Gow [15] in horizontal thin sections of young, primarily columnar sea ice. It is also observed that  $\alpha = 1$  gives a good fit for the range of volume fractions covered here, and consequently we use this value for all the numerical calculations in this work. Once  $\alpha$  is determined, the other parameter  $\mu$  is solved by the matching condition  $E[A] = \langle A \rangle$  as above. Throughout this study  $n = m = 1024$ .

Also as observed in Refs. [7,8,16], brine inclusions in columnar sea ice become connected on macroscopic scales only when the brine volume fraction exceeds around 5%. To reflect this behavior, we allow some randomly selected tubes to be disconnected from the system in an effort to simulate the disconnection of brine inclusions. Since the dominant conduction direction is the vertical direction, we introduce a probability of disconnection for vertical tubes only, consistent with the X-ray tomographic data and pore structure analysis in Refs. [8,16], and this constitutes an additional input to the model.

We proceed to perform numerical simulations for  $\sigma_v^*$  with several situations described by the brine volume fraction, and the corresponding microstructure summarized from our data. For each value of  $\phi$ , we choose an appropriate probability of disconnection to differentiate the microstructure from the others. The brine conductivity  $\sigma_b$  in fact depends on the temperature and the salinity of the sea ice, which characterize the state of the sea ice at the particular level of brine volume fraction. For this study, in order to focus on the effects of the brine volume fraction, we assume a fixed value for the salinity  $S = 7$  ppt. We then invert the Frankenstein–Garner relation [4] to obtain

$$T = -\frac{49.185}{\frac{1000\phi}{S} - 0.532}, \quad (15)$$

which is then substituted in the Stogryn–Desargant relation [18]

$$\sigma_b = -T \cdot e^{0.5193 + 0.08755T}, \quad T \geq -22.9^\circ\text{C}, \quad (16)$$

to determine the brine conductivity for the sea ice at a particular brine volume fraction  $\phi$ . The values of temperature and brine conductivity, as well as the probabilities of disconnection that describe one important aspect of the microstructure, are listed in Table 1 for selected values of the brine volume fraction for which we perform numerical simulations in this work. We also use an average pure ice conductivity value of  $\sigma_{ice} = 1.1 \times 10^{-8}$  at a temperature  $T = -10^\circ\text{C}$ . Here all the conductivity quantities have the unit  $\text{Ohm}^{-1} \text{m}^{-1}$ .

In Fig. 2, we plot the values of the effective vertical conductivity  $\sigma_v^*$  and form factor  $\sigma_v^*/\sigma_b$  from our measured data sets and compare with the results of the network model. First we note that our assumption  $\sigma_{ij}^v = \sigma_{ij}^h = \sigma_b$  simplifies Eq. (5) such that the solution  $\Phi$  is independent of  $\sigma_b$ . This allows us to separate the effects of decreasing  $\sigma_b$  and increasing  $\sigma_v^*$  as  $\phi$  increases. As we see from the graphs for both the effective vertical conductivity and the form factor, our results show close agreement with the measurements. In Fig. 2(a), the simulated curve is consistent with

**Table 1**  
Numerical parameters used in simulation.

$\phi$ (%)	2.5	5.0	7.5	10.0	12.5
$P_{\text{disconnect}}$	0.9	0.7	0.5	0.25	0
$T$ ( $^\circ\text{C}$ )	-16.18	-7.44	-4.83	-3.58	-2.84
$\sigma_b$ ( $\text{Ohm}^{-1} \text{m}^{-1}$ )	6.596	6.519	5.319	4.395	3.722

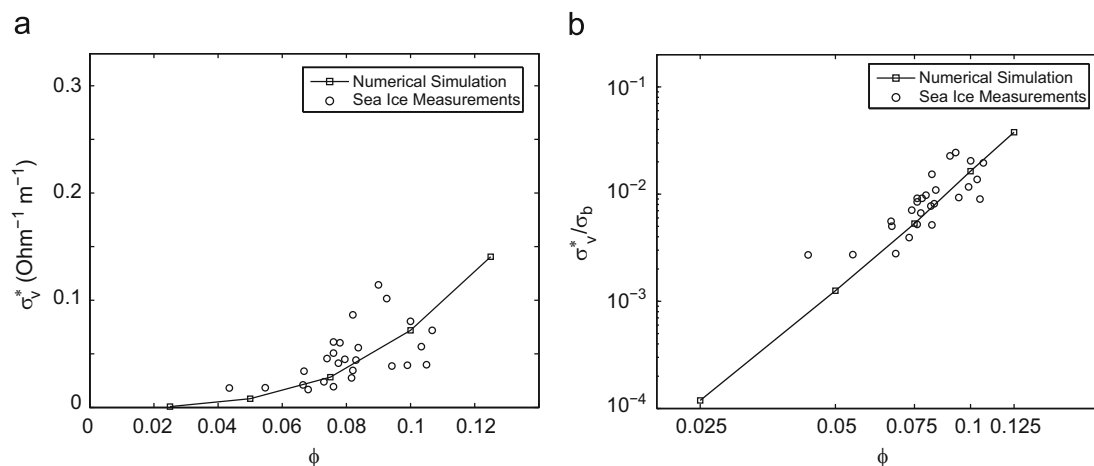


**Fig. 2.** (a) Data on the vertical conductivity of first year Antarctic sea ice is compared with the results of numerical simulations and (b) data on the form factor is compared with numerical results from the network model, and displayed on a logarithmic scale.

critical behavior in a finite volume. For the form factor comparison in Fig. 2(b), we choose a log–log scale to detect any linear behavior, which would suggest Archie's law behavior. As demonstrated in this log–log graph, such a power law could also be developed from this network model. These results are consistent with the behavior found for the fluid permeability in Ref. [8]. In Ref. [9] we use percolation theory and other methods to analyze our vertical conductivity data.

#### 4. Conclusions

We have developed a network model for the vertical conductivity of sea ice. The model incorporates statistical information about the brine microstructure, through a lognormal distribution describing the temperature dependence of the inclusion sizes, and connectivity information obtained from X-ray CT data. The model agrees well with field data for Antarctic sea ice. Our work will aid in measurements of sea ice thickness which depend on knowledge of its electrical properties.

#### Acknowledgements

We are grateful for the support provided by the Division of Mathematical Sciences, the Division of Atmospheric Sciences, and the Arctic Natural Sciences Program at the US National Science Foundation (NSF). We also thank T. Worby, J. Reid, the Australian Antarctic Division and the crew of the *Aurora Australis* for their support of our work during the SIPEX Antarctic expedition. Adam Gully gratefully acknowledges the support of the NSF Research Experiences for Undergraduates (REU) Program and an NSF VIGRE graduate fellowship, and Christian Sampson gratefully acknowledges support from the NSF REU Program.

#### References

- [1] C. Bock, H. Eicken, *Ann. Glaciol.* 40 (2005) 179.
- [2] R.G. Buckley, M.P. Staines, W.H. Robinson, *Cold Reg. Sci. Tech.* 12 (1986) 285.
- [3] H. Eicken, Growth, microstructure and properties of sea ice, in: D.N. Thomas, G.S. Dieckmann (Eds.), *Sea Ice: An Introduction to its Physics, Chemistry, Biology and Geology*, Blackwell, Oxford, 2003, pp. 22–81.
- [4] G. Frankenstein, R. Garner, *J. Glaciol.* 6 (48) (1967) 943.
- [5] K. Fujino, Y. Suzuki, *Low Temp. Sci. A* 21 (1963) 151.
- [6] K.M. Golden, *Not. Amer. Math. Soc.* 56 (5) (2009) 562.
- [7] K.M. Golden, S.F. Ackley, V.I. Lytle, *Science* 282 (1998) 2238.
- [8] K.M. Golden, H. Eicken, A.L. Heaton, J. Miner, D. Pringle, J. Zhu, *Geophys. Res. Lett.* 34 (2007) L16501 (6 pages and issue cover), doi:10.1029/2007GL030447.
- [9] K.M. Golden, A. Gully, C. Sampson, J. Zhu, A.P. Worby, J. Reid, Theory and measurements of electrical conductivity in Antarctic sea ice, *Deep Sea Res.* (2009), submitted.
- [10] K.M. Golden, A.L. Heaton, H. Eicken, V.I. Lytle, *Mech. Mat.* 38 (2006) 801.
- [11] C. Haas, *Cold Reg. Sci. Tech.* 27 (1998) 1.
- [12] C. Haas, Dynamics versus thermodynamics: the sea ice thickness distribution, in: D.N. Thomas, G.S. Dieckmann (Eds.), *Sea Ice: An Introduction to its Physics, Chemistry, Biology and Geology*, Blackwell, Oxford, 2003, pp. 82–111.
- [13] C. Haas, *Geophys. Res. Lett.* 31 (2004) L09402, doi: 10.1029/2007GL030447.
- [14] C. Haas, S. Gerland, H. Eicken, H. Miller, *Geophysics* 62 (1997) 749.
- [15] D.K. Perovich, A.J. Gow, *J. Geophys. Res.* 101 (C8) (1996) 18,327.
- [16] D.J. Pringle, J.E. Miner, H. Eicken, K.M. Golden, *J. Geophys. Res.* C 114 (2009) C12017 (14 pages), doi:10.1029/2008JC005145.
- [17] J.E. Reid, A. Pfaffling, A.P. Worby, J.R. Bishop, *Ann. Glaciol.* 44 (2006) 217.
- [18] A. Stogryn, G.J. Desargant, *IEEE Trans. Antennas Propagat.* AP-33 (5) (1985) 523.
- [19] F. Thyssen, H. Kohlen, M.V. Cowan, G.W. Timco, *Polarforschung* 44 (1974) 117.
- [20] G.W. Timco, *J. Glaciol.* 22 (1979) 461.
- [21] W.F. Weeks, S.F. Ackley, The growth, structure and properties of sea ice, in: N. Untersteiner (Ed.), *The Geophysics of Sea Ice*, Plenum Press, New York, 1986, pp. 9–164.
- [22] A.P. Worby, P.W. Griffin, V.I. Lytle, R.A. Massom, *Cold Reg. Sci. Tech.* 29 (1999) 49.
- [23] J. Zhu, A. Jabini, K.M. Golden, H. Eicken, M. Morris, *Ann. Glaciol.* 44 (2006) 129.